THE JOURNAL OF PHYSICAL CHEMISTRY C

Article

pubs.acs.org/JPCC

Coverage-Dependent Interactions at the Organics−Metal Interface: Quinonoid Zwitterions on Au(111)

Scott Simpson,[†] Donna A. Kunkel,[‡] James Hooper,[†] Justin Nitz,[‡] Peter A. Dowben,[‡] Lucie Routaboul,[§] Pierre Braunstein,[§] Bernard Doudin,[∥] Axel Enders,*[,‡] and Eva Zurek*[,†]

[†]Department of Chemistry, State University of New York at Buffalo, Buffalo, New York 14260-3000, United States

[‡]Department of Physics and Astronomy, University of Nebraska—Lincoln, 855 North 16th Street, Lincoln, Nebraska 68588, United States

[§]Laboratoire de Chimie de Coordination, Institut de Chimie (UMR 7177 CNRS), Universite de Strasbourg, 4 rue Blaise Pascal, 67081 Strasbourg, France

[∥]Institut de Physique et Chimie des Materiaux de Strasbourg (IPCMS UMR 7504 CNRS) and Lab of Nanostructures in Interactions with their Environment (NIE), Universite de Strasbourg, 23 Rue du Loess, 67034 Strasbourg, France

Supporting Information

ABSTRACT: The large intrinsic electric dipole of about 10 D of a *p*-benzoquinonemonoimine compound from the class of *N*-alkyldiaminoresorcinone (or 4,6-bisdialkylaminobenzene-1,3-diones, i.e., $C_6H_2(\cdots NHR)_2(\cdots O)_2$, where R = H) zwitterions is reduced considerably upon adsorption on Au(111) substrates. Scanning tunneling microscopy images reveal parallel alignment of adsorbed molecules within extended islands, leading to the formation of polarized domains. This is in contrast to the typical antiparallel alignment found in the bulk. High-resolution images show that the molecules form rows along the ⟨101⟩ directions of the Au(111) surface, but otherwise their arrangement is only weakly perturbed by the Au(111) $(23 \times \sqrt{3})$ herringbone surface reconstruction. Density functional theory calculations show that upon increasing the molecular density the strength of the interaction between the zwitterions and the Au(111) surface decreases. Thus, the charge redistribution, which occurs at the interface as a result of molecular adsorption, and therefore the interfacial dipole is coverage dependent. The weakening of the interaction at the organic−metal interface with increasing coverage is experimentally observed as a contraction of the intermolecular bond length. Moreover, it is the strong adsorbate−adsorbate interactions (and not the interactions between the adsorbate molecules and the surface) which determine the molecular arrangement within the 2D network the zwitterions form.

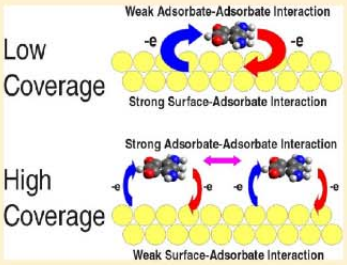

Organic molecules often exhibit electronic properties that are similar to semiconductors and offer additional flexibility for controlling those properties through structural design and manipulation of interactions with supporting substrates, adsorbates, and functional groups. Such great potential is currently at the origin of a rapidly growing and rapidly diversifying branch of molecular electronics based on carbon-based polymers and small molecules.[1−3] A key parameter, and often a hindrance to better device operation, for all organics-based electronics is the electrostatic charge injection barrier, related to the electrostatic landscape that develops on surfaces and interfaces and generally impedes charge transfer. These charge barriers at electrode interfaces can be manipulated with inorganic adsorbates if the adsorbate's work function is lower than that of the surface. Importantly, organic molecules can exhibit intrinsic charge dipoles and are therefore potentially useful to manipulate charge barriers at surfaces and interfaces as needed, if the current fundamental, molecular-level understanding of the material properties is improved through basic research.

Currently existing experimental and theoretical studies dealing with adsorbed molecules with intrinsic dipoles typically focus on the competition of dipole−dipole interactions between the molecules with other bonding forces and how such competition determines the molecular self-assembly.[4] For instance, the dipole moment of anthraquinone compounds was found to play a role in the bonding to Cu(111) and the formation of dimers.[5] As another example, the comparatively small dipole moment present in styrene in the gas phase increases upon adsorption through interactions with the surface.[6] The in-plane dipole moment is even found to force the formation of small rings which serve to cancel the electrostatic stray field.[6] At higher coverage, the styrenes form domains of parallel aligned molecules, which have also been attributed to their dipole moment interactions.[7] Dipole−dipole interactions can also alter the net force between adsorbed

Received: April 5, 2013
Revised: July 6, 2013

   dx.doi.org/10.1021/jp403384h | *J. Phys. Chem. C* XXXX, XXX, XXX XXX

molecules from repulsive to attractive, as has been shown, for instance, with the salen complexes on Cu(111).[8] While charge exchange between molecules and supporting substrates seems to represent the main mechanism that determines the resulting dipole of the adsorbed molecules, other contributions, such as image dipoles, can also play a role.[9] Small molecules with large intrinsic dipoles are therefore well-suited model materials for investigating more systematically how the intrinsic molecular dipole evolves and possibly governs surface adsorption.

We have recently investigated a newly discovered class of molecules with unusually strong intrinsic dipoles, which are the *p*-benzoquinonemonoimine zwitterion (Z1), $C_6H_2(\cdots NHR)_2(\underline{\cdots} O)_2$.[10,11] Molecules with R = H are considered as the parent molecule of an entire family, and numerous derivatives have been prepared with other R substituents. The electrically neutral molecules carry positive and negative charges on opposite parts of the central ring, the positive charge being delocalized between the nitrogen moieties over four bonds involving 6π-electrons, while the negative charge is likewise spread between the oxygen atoms. This electronic structure results in a large dipole moment of approximately 10 D.[10] In the crystalline state, the zwitterions form molecular arrangements whose structures are thought to be determined by their strong dipole and by the H-bonding intermolecular interactions involving the O and N−H groups of adjacent molecules.[10−13] The dipoles of neighboring molecules tend to point in opposite directions in the bulk crystals, thus effectively canceling out the dipole and reducing the electrostatic energies.[10−13] Similar antiparallel alignment is observed on HOPG surfaces in solution.[14] Under UHV conditions on Ag(111) and Cu(111) surfaces, surface interactions play a deterministic role in what self-assembled structures quinonoid zwitterions form.[15]

The molecular interactions with Au are of considerable practical importance as gold is commonly used as a contact component in devices and has been shown to interact substantially with organics.[16] For this reason, we expand here our studies of organics-induced interface dipoles to include the close-packed Au(111) substrate. Crystalline Au substrates exhibit comparatively complex (111) surfaces because of the tendency for this close-packed surface to exhibit a large number of reconstructions, most notably the $(23 \times \sqrt{3})$ herringbone surface reconstruction.[17−20] In spite of the greater complexity of the Au(111) surface over the Cu(111) or Ag(111) surfaces, many studies find adsorbate−substrate interactions to be comparatively weak on Au(111). The focus here is on studying how the interaction of the zwitterions changes as a function of molecular density, which is varied by changing the surface coverage in our calculations.

With notable exceptions, i.e., refs 39, 21, and 22, recent studies investigating thin organic films on transition metal surfaces infer thin-film properties from the computation of a single molecule on a metal slab, which often corresponds to an idealized system of "isolated" molecules.[23,25−27] Here, we present calculations where we systematically vary the molecular density and in so doing illustrate that the interaction of organics in a 2D island with the substrate differs from that of an isolated molecule. We show that for low coverages the charge transfer that occurs upon adsorption leads to a surface dipole which attempts to cancel out the molecular dipole, similar to what was found earlier for Ag(111) and Cu(111) substrates.[39] This electronic reorganization alters the system's dipole considerably. At higher coverages the decrease of the bonding strength between the substrate and the adsorbate results in an increase of the intermolecular attraction. Because of this, as the coverage increases, the distance between adjacent zwitterions decreases, with a concomitant increase in the adsorbate to substrate distance. This leads to a decrease in the overlap between molecular and surface wave functions, which markedly affects the charge redistribution occurring upon adsorption, and the induced surface dipoles.

■ EXPERIMENTAL METHODS

An Omicron low-temperature scanning tunneling microscope (STM) with an electrochemically etched W tip was used under UHV conditions to image the samples. The Au(111) substrate was prepared in situ by repeated cycles of Ar ion sputtering and subsequent annealing at approximately 600 °C. The sample was imaged with STM to confirm cleanliness before molecules were deposited. The molecules were synthesized as described in refs 10, 11, 13, and 28. In the vacuum system, the molecules were thermally evaporated from a Knudsen cell onto the Au sample held at room temperature, at a rate of about 0.03 monolayers (ML) per minute. After deposition, the sample was transferred in situ into the STM and imaged at a sample temperature of 77 K. Measurements were always taken over the distance of several molecules to reduce the measurement error. Especially at low coverages, the measurements were performed on small islands such as those in Figure 1(a) where we were able to measure

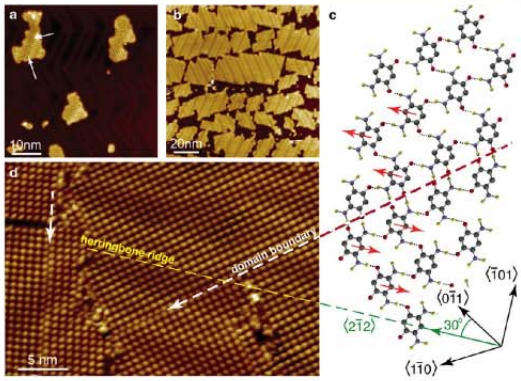

Figure 1. Low-coverage STM image (a) and high-coverage STM image (b) of parent quinonoid zwitterions on Au(111). Tunneling parameters: U_b = 0.3 V, I_t = 750 pA. (c) Proposed structure model of parent zwitterions on Au(111). (d) High-resolution STM image showing details of the molecular network, together with the herringbone reconstruction ridges (U_b = 0.3 V, I_t = 900 pA). Structural domain boundaries are highlighted with white arrows in (a) and (d). Red arrows indicate the orientation of the electric dipole moment on selected molecules in (c).

over several molecules in the interior of an island, while neglecting molecules within proximity of the island edges. Thus, structural relaxation effects near the island edges were excluded from the measurements. Further, measurements were repeated on many islands and several samples, with varied scan angles and speed, to minimize systematic experimental errors.

■ COMPUTATIONAL METHODS

Density functional theory (DFT) calculations (geometry optimizations, electronic densities of states, charge densities)

dx.doi.org/10.1021/jp403384h | J. Phys. Chem. C XXXX, XXX, XXX XXX

were performed using the Vienna Ab initio Simulation Package (VASP) version 5.2.11.[29] The projector augmented wave (PAW) method[30] was used to treat the core states along with a plane-wave energy cutoff of 500 eV, and the C/N/O 2s/2p, H 1s, and Au 6s/5d electrons were treated explicitly. The nonlocal correlation functional of Langreth and Lundqvist (vdW-DF2)[31,32] was employed to account for the dispersion interactions. The Γ-centered Monkhorst−Pack scheme was used to generate *k*-point grids for various coverages which varied from 0.96 (7 × 7 × 1), 0.89 (19 × 19 × 1), 0.64 (11 × 11 × 1), 0.50 (7 × 7 × 1), 0.32 (7 × 7 × 1), 0.22 (7 × 7 × 1), to 0.16 ML (3 × 3 × 1). These grids were also used for calculations on the bare hexagonal Au(111) surface slabs and the corresponding gas-phase networks. Further structural information about the unit cells used for the different coverages can be found in the Supporting Information (SI). The computational settings employed gave rise to energies converged to within 4 meV/atom, and the geometries were converged such that the magnitude of the largest force acting on the optimized atoms was less than 0.05 eV/Å. The surface was simulated using a four-layer slab, with a ∼30 Å vacuum separating two slabs. During the geometry optimizations the bottom two layers were fixed at the experimental bulk lattice constant of 4.08 Å for Au, whereas the upper two layers of the surface and the molecule were free to fully relax. The optimal lattice constant calculated with vdW-DF2 is 4.35 Å. In the SI we illustrate that the trends observed for calculations using this lattice constant instead are in agreement with those obtained using the experimental value. The dipole correction was applied along the direction perpendicular to the metal surface. The "free" zwitterion was optimized in a box measuring (28.838 × 28.838 × 40) Å, and a Γ-point grid was sufficient to achieve convergence.

RESULTS AND DISCUSSION

Experimental Results. A series of STM images of parent zwitterions on Au(111) at a variety of coverages are shown in Figure 1. The molecules form 2D islands of structurally ordered networks on the Au(111) surface. Island nucleation occurs preferentially at the kink sites of the well-known herringbone reconstruction,[19,20] which is clearly visible in the STM images in Figure 1. The reconstruction does not impede island growth with increasing coverage. At a coverage below 0.1 ML few islands containing approximately 50−200 molecules are visible (see Figure 1a). The observation of a low frequency of occurrence of nucleation events relates to a large mean free path for the adsorbed zwitterions, which also implies low diffusion barriers. As the adlayer coverage increases, the islands grow in size, extending easily over many "herringbone" reconstruction ridges.

It becomes obvious at higher coverage that the orientation of the islands correlates with the local direction of the herringbone ridges. Especially, Figure 1b and d shows the organic network with molecular resolution, together with the herringbone reconstruction. Atomically resolved STM images of the uncovered Au(111) were also taken on the same sample on uncovered surface areas, to identify the crystallographic ⟨110⟩ directions of the surface and their alignment with respect to the observed molecular rows.

The structural model shown in Figure 1c results from a close inspection of the alignment of the molecular rows in the networks, the orientation of those rows with respect to the reconstruction ridges as well as the ⟨110⟩ directions of the Au surface, and the details of the geometry at the structural domain boundaries. The basis of our model is that within the islands the two enamine/iminium groups of each molecule bind to the oxygen moieties of two neighboring molecules via hydrogen bonds, thus creating a 2D network exhibiting a nearly square-shaped unit cell. This bonding scheme assumes parallel alignment of the molecular dipole moments within each island, so that the islands must exhibit remnant nonzero electric polarization. Boundaries between the resulting structural and polar domains are frequently observed, such as those highlighted by white arrows in Figure 1a,d. The boundaries can be easily constructed from the proposed model by assuming two structural domains, aligned in opposite directions with respect to each other. Pairs of molecules directly at the boundary form double hydrogen bonds as shown in Figure 1c, and this would tend to stabilize the domain boundary and is also consistent with the observed bonding on HOPG[14] and Cu(111).[15]

It is concluded from this model that (i) rows of molecules align with the in-plane ⟨101⟩ directions of Au, (ii) the symmetry axis of the molecules is aligned parallel to the reconstruction ridges, which explains the observed tilt of the islands in Figure 1b, and (iii) that the symmetry axes of the molecules make an angle of 30° with the ⟨011⟩ directions of the Au surface by following the herringbone ridges, which are known to make such an angle with the densely packed directions of the surface.[19,20]

We measured the intermolecular spacings with subangstrom precision, to identify the exact adsorption sites on the Au(111) surface. We find that the molecular spacing along the ⟨101⟩ direction of the Au is within the range of 1.08 and 1.11 nm. This spacing would be commensurate with the lattice spacing of the Au surface along this densely packed direction, where four atomic distances correspond to 1.15 nm, if a compression of the surface in this direction of 5% is considered. Such a compression along ⟨101⟩ is indeed assumed to be the origin of the surface reconstruction.[20] The same measurements of the molecule spacings in the perpendicular ⟨212⟩ direction show, however, that here the molecular positions are incommensurate with the Au surface lattice. This means that although the ⟨110⟩ surface directions of the Au surface are a template for the growth of molecular rows the molecules are not generally locked to specific adsorption sites on the surface. This also implies very small binding energy variations between on-top, bridge, and hollow sites for the molecules on the surface.

The same analysis of the intermolecular bond length was performed for comparison at low (≈0.1 ML) and high (≈0.8−1.0 ML) molecular coverage. Figure 2a compares two typical line scans taken over five molecules within a low coverage island and a high coverage film. Histograms of all measurements taken at both coverages, together with Gaussian fits, are shown in Figure 2b. Comparison of both histograms shows unambiguously that the intermolecular bond length contracts by 0.2 Å upon increasing the coverage from 0.1 ML to a nearly complete monolayer.

Given the ubiquitous nature of polarization-induced renormalization of molecular levels at metallic surfaces,[33] the electric dipole of the zwitterions on Au(111) is expected to be significantly altered as compared to isolated species. Density functional theory calculations were therefore carried out to study the bonding of an "isolated" zwitterion to Au(111) and to explore the variation of the binding energy and charge

dx.doi.org/10.1021/jp403384h | J. Phys. Chem. C XXXX, XXX, XXX XXX

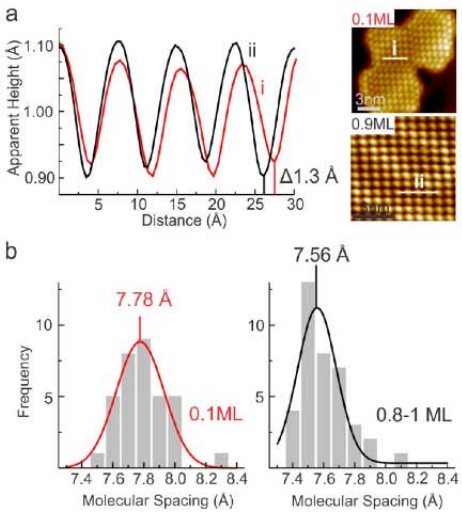

Figure 2. (a) STM images and representative line profiles of parent zwitterions taken at low (i) and high (ii) coverages as indicated. (b) Histograms of length measurements taken for low and high coverages, fitted with a Gaussian curve.

redistribution which occurs upon adsorption as a function of surface coverage.

Geometries and Binding Energies. First-principles calculations have been undertaken to gain a molecular-level understanding of the interaction of the parent zwitterion with the Au(111) surface, the charge transfer which occurs at the interface, and the dependence of these properties upon the coverage. Periodic calculations with plane-wave basis sets were carried out where the Langreth and Lundqvist method (vdW-DF2[31,32,34]) was used to account for the van der Waals interactions. The vdW-DF and vdW-DF2 methods have been applied to a broad range of systems, including benzene on Cu(111),[35] dichlorobenzene on Au(111) and (332),[23] various amines on Au(111),[24] as well as noble gases[36] and H_2[37] on various metal surfaces. Even though this functional performs better than standard generalized gradient approximation (GGA) type functionals for systems where dispersion interactions are of import, it can in some cases underestimate the equilibrium binding energies between organic molecules and surfaces.[38] For example the binding energy of benzene to Au(111) and Ag(111) has been calculated as being 0.56[26] and 0.39 eV,[39] respectively, as compared to the experimental estimates of 0.64[40] and 0.57 eV,[41] suggesting that the interaction energies we calculate may be up to 32% too small. The accurate treatment of dispersion interactions between organic molecules and metal surfaces is a challenging task and the topic of numerous recent theoretical studies.[25,42,43] For example, it has recently been shown that the binding energies of benzene on Au(111) and Pt(111) calculated with the optB88-vdW and PBE+vdW^{surf} methods are closer to experiment than those obtained using vdW-DF2.[26]

To investigate the interaction of flat-lying orientations of the zwitterion with the substrate, geometry optimizations were carried out where the center of the molecule was placed over the top (T), bridge (B), or hollow (H) position of the Au(111) surface, as illustrated in Figure 3. In addition two configurations

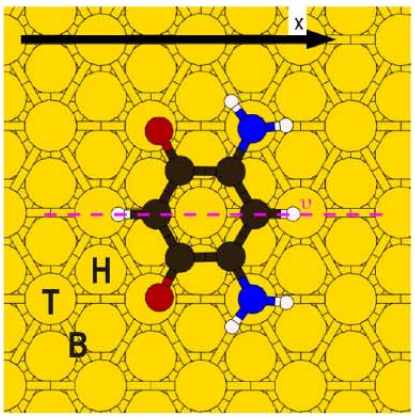

Figure 3. Au(111) surface indicating the top (T), hollow (H), and bridging (B) sites. The axis that bisects the zwitterion, ν, is indicated by the pink dashed line and the x-axis by the black arrow. In this figure the zwitterion is centered over the T site with $\theta = 0°$. Carbon, nitrogen, oxygen, hydrogen, and gold atoms are colored as black, blue, red, white, and yellow, respectively.

were considered: one where the axis bisecting the zwitterion (ν) makes an angle (θ) of 0° with respect to the x-axis and another where this angle is 30°. The binding energy of the most stable configuration, H0°, was calculated as being 0.98 eV. The relative binding energies with respect to the most stable site (see Table 1) show that the potential energy surface is quite

Table 1. Adsorption Sites, Angles (θ) (see Figure 3 for an Illustration of the Binding Sites), and the Metal to Adsorbate Distances ($d_{ZI\text{-}surf}$) of the Quinonoid Zwitterion on the Au(111) Surface[a]

site	θ	E_{rel} (eV/molecule)	$d_{ZI\text{-}surf}$ (Å)
B	0	0.01	3.26
B	30	0.03	3.39
H	0	0.00	3.25
H	30	0.04	3.38
T	0	0.03	3.20
T	30	0.04	3.25

[a] $d_{ZI\text{-}surf}$ was taken as the shortest vertical distance between a carbon atom in the zwitterion and a gold atom on the surface.

flat, with around 0.04 eV corrugation, which is similar to results previously obtained for benzene on various coinage metal surfaces.[26,35] The small differences in energy imply that the diffusion barrier is low. The shortest vertical distance between a carbon atom in the ring and the metal surface was found to be 3.25 Å, and the zwitterion remains relatively parallel to the metal surface after optimization. This computational result of only weak corrugation of the potential energy surface is consistent with the experimental observation of a long mean free path of the adsorbed molecules and an organic adlayer that is incommensurate with the substrate (see the previous section).

The computations above were performed using a coverage of 0.555 molecules/nm^2. Our STM images (see for example Figure 1d) revealed that one monolayer of coverage corresponds to 1.73 ± 0.1 molecules/nm^2. Thus, the coverage

dx.doi.org/10.1021/jp403384h | J. Phys. Chem. C XXXX, XXX, XXX XXX

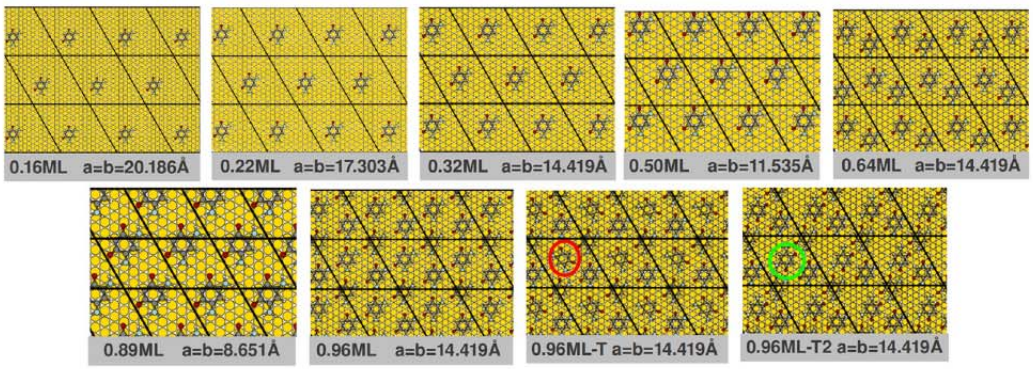

Figure 4. Illustration of the zwitterionic networks which were optimized on the Au(111) surface at coverages ranging from 0.16 to 0.96 ML, where 1 ML was defined as being 1.73 molecules/nm^2. The unit cells are indicated by the black lines, and the length of the lattice vectors, *a* and *b*, is provided. The bottom row of 0.96 ML configurations differs by a rotation of one ZI per unit cell by 90° (T) and 180° (T2). In each of these configurations one of the rotated ZI molecules is highlighted by a red or green circle.

employed for the study of "isolated" systems corresponds to 0.32 ML. It should be emphasized here that the molecular arrangement employed in the computations in the low coverage regime is different from the experimentally observed island formation. The goal of the theoretical analysis is, however, to establish how changing the intermolecular spacing (through a systematic change in the coverage) affects the interaction of the zwitterions with the Au(111) surface. The highest coverage considered for the calculations provided in the main text was 1.67 molecules/nm^2 (0.96 ML). As will be shown, the adsorption energy for the lowest coverages considered, 0.16 ML, was roughly equivalent to the one computed for 0.32 ML. Also, the interaction between the zwitterions in the 0.32 ML network was found to be negligible, verifying that this computational model was a good approximation for an isolated molecule.

In Figure 4 we illustrate the unit cells which were considered in the coverage studies. With the exception of two of the 0.96 ML configurations, the molecules have been arranged in such a way so that they form rows within which all of the dipoles point in a single direction. The oxygen atoms in one such row are oriented to face toward the amine groups in the next one, so that the negative end of the dipole within one row points toward the positive end of the dipole in the adjacent one (a "head-to-tail" arrangement). At low coverage, the molecules interact with each other via long-range dipole−dipole interactions. As the coverage increases intermolecular hydrogen-bonding and dispersion forces become increasingly important. For this reason, and inspired by our experimental observations at high coverage, the molecules have generally been positioned in such a way as to allow for hydrogen bonding, provided that the distance between the rows is small enough. The 0.64 ML coverage can be thought of as a honeycomb network, and putting one more molecule in the center of the hexagons increases the coverage to 0.96 ML. Three such high-coverage networks have been considered: in the first (0.96 ML) the staggered rows of aligned zwitterions resemble those in a single domain of the structure model, illustrated in Figure 1c, despite their differing coordination environments. The second (0.96 ML-T) can be obtained by rotating the central zwitterion (circled in red), and therefore its dipole, by 90°; the third (0.96 ML-T2) is constructed by a 180° rotation of the zwitterion (circled in green) instead. Optimization of the 0.96 ML network in the gas phase resulted in a negligible geometrical distortion, indicating that this is the preferred interatomic spacing within a flat layer of gas-phase zwitterionic molecules (for this particular unit cell).

The binding energies (BEs) of the various organic networks shown in Figure 4 are given in Table 2. The binding energy was computed as the difference in electronic energy between the total system and the sum of its fragments in accordance with eq 1

$$\mathrm{BE} = \frac{1}{M}[-E_{\mathrm{ZI\text{-}surf}} + [M \times E_{\mathrm{ZI}}] + E_{\mathrm{surf}}] \quad (1)$$

where the first term, $E_{\mathrm{ZI\text{-}surf}}$, is the energy of the total surface−adsorbate system; the second term is the energy of an isolated zwitterion; *M* is the number of molecules per unit cell; and the third term is the energy of the periodic Au(111) slab.

It is useful to decompose the overall binding energy into two contributions

$$\mathrm{BE} = \frac{1}{M}[\mathrm{BE}_{\mathrm{ZI\text{-}ZI}} + \mathrm{BE}_{\mathrm{ZI\text{-}surf}}] \quad (2)$$

Table 2. Influence of the Surface Coverage on the Binding Energy (BE), Contributions to the Binding Energy (see Equation 2), and the Metal to Adsorbate Distance ($d_{\mathrm{ZI\text{-}surf}}$) of the Quinonoid Zwitterion on the Au(111) Surface[a]

coverage (ML)[b]	BE (eV/molecule)	$\mathrm{BE}_{\mathrm{ZI\text{-}ZI}}$ (eV/molecule)	$\mathrm{BE}_{\mathrm{ZI\text{-}surf}}$ (eV/molecule)	$d_{\mathrm{ZI\text{-}surf}}$ (Å)
0.96-T2	1.29	0.48	0.81	3.36
0.96-T	1.14	0.52	0.62	3.36
0.96	1.47	0.73	0.74	3.44
0.89	1.04	0.24	0.80	3.34
0.64	1.19	0.42	0.77	3.37
0.50	1.02	0.07	0.96	3.27
0.32	0.98	0.04	0.95	3.25
0.22	1.01	0.02	0.99	3.26
0.16	0.98	0.01	0.97	3.26

[a]The orientations of the molecules at these coverages are illustrated in Figure 4. [b]One ML of coverage is defined as 1.73 molecules/nm^2.

dx.doi.org/10.1021/jp403384h | J. Phys. Chem. C XXXX, XXX, XXX XXX

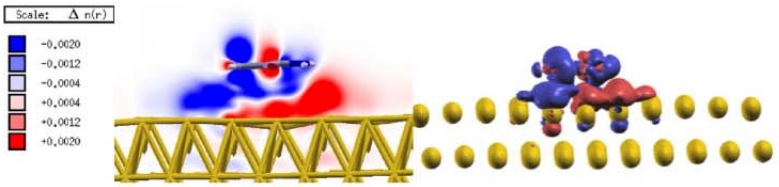

Figure 5. Redistribution of electronic charge which occurs upon adsorption of the zwitterion to the Au(111) surface for a coverage of 0.16 ML. Red indicates an accumulation and blue a depletion of charge. (left) A two-dimensional plot of the CDD which shows a slice bisecting the molecule. The amine ends are pointed toward the right. The inset shows the color scheme associated with the isovalues in units of $e/Å^3$. (right) An isosurface of the CDD with isovalue ± 0.002 $e/Å^3$.

where the first term is the difference in energy between the zwitterionic network (in the geometry optimized on the surface) and that of the free, isolated zwitterion and the second term is the adsorption energy of the network to the Au(111) surface.

Table 2 shows that for coverages up to 0.50 ML the interaction between the zwitterionic network and Au(111) remains nearly constant and close to the value calculated for the lowest coverage considered, 0.16 ML. The small deviations in $BE_{ZI\text{-}surf}$, which range from 0.95 to 0.99 eV/molecule, are likely a result of the corrugations in the potential energy surface which we estimate to be ~0.04 eV/molecule based upon the results of our binding site studies. As a result of the nearly negligible intermolecular interaction, and the almost constant adsorption energy, the binding energy remains virtually unchanged for a coverage of 0.50 ML or less.

$BE_{ZI\text{-}ZI}$ is small for low coverages and increases as the intermolecular distance decreases because of the variation in intermolecular hydrogen bonding and dipolar interactions between the rows of molecules within the simulation cells (see Figure 4). The influence of the rotated dipole within the three 0.96 ML coverage structures will be discussed in greater detail below. The strengthening of the intermolecular interactions also results in a decrease of $BE_{ZI\text{-}surf}$. In general, these two opposing trends lead to a gradual increase in the net binding energy with increasing coverage for the zwitterionic networks considered. This behavior is in stark contrast to the one calculated for tetrathiafulvalene adsorbed to Au(111), where the overall adsorption energy decreased with increasing coverage.[21] Fraxedas and co-workers[21] attributed this trend to the repulsion between neighboring dipoles, which became larger as the distances between the tetrathiafulvalene molecules became smaller. Another theoretical study has shown that the pattern which rubrene forms on Au(111) can be explained via a simple model consisting of long-range repulsive dipolar forces and attractive van der Waals interactions at shorter distances.[44] In line with our work, it has been illustrated that the intermolecular interactions between 1,4-diaminobenzene (BDA) molecules on Au(111) are important in understanding the patterns formed upon molecular adsorption.[24]

However, the trends noted above are not linear, and two significant outliers emerge upon careful examination of Table 2. The net binding energies calculated for the 0.64 ML and the 0.96 ML coverages are significantly greater than what would be expected based upon an extrapolation of the binding energies of the other networks we have considered, primarily as a result of the stronger intermolecular attraction. Moreover, even though the molecular density is larger for the 0.89 ML coverage, it has a smaller $BE_{ZI\text{-}ZI}$ than the 0.64 ML, honeycomb-like network. This is due, in part, to the less favorable intermolecular interactions within the ZI rows in the former; the molecules rotate by ~30° when the ZI network is isolated and optimized in the gas phase. What is even more striking is that placing a zwitterion in the hexagonal holes of the 0.64 ML arrangement yields a dramatic increase in $BE_{ZI\text{-}ZI}$ to 0.73 eV/molecule. In going from 0.64 to 0.96 ML the binding energy between the Au(111) and the zwitterions decreases, with a concomitant increase in the distance between the two. Nonetheless, the total binding energy calculated for the 0.96 ML coverage is 0.28 eV/molecule larger than any of the other systems we have considered, and the local environment about each zwitterion matches well with the structural model proposed for the molecules within a single domain (see Figure 1c). About half of the total binding energy for the 0.96 ML network is a result of the attractive intermolecular interactions, highlighting the importance of the molecular arrangement in optimizing the hydrogen bonding, dipole−dipole, and van der Waals bonding between the zwitterions. It is noted that the unit cell used in the computation contains only one structural domain and does not have a region representative of a domain boundary.

Comparison of the three 0.96 ML networks illustrates that it is not only the coverage and pattern but also the orientation of the zwitterions which determine their stability. The 0.96-T2 is higher in energy by approximately 0.18 eV/molecule due to the decrease in the intermolecular bonding strength (note that $BE_{ZI\text{-}surf}$ is actually greater than in the unturned configuration). The 0.96-T is even less stable, such that the change in energy which results from rotating one of the ZI molecules in the 0.96 ML configuration, i.e., in going from 0.96 to 0.96-T to 0.96-T2, was determined as being ~0.33 eV/molecule. The stability of the unturned network (in which the dipoles of the zwitterions are aligned in a "head-to-tail" fashion) can in part be explained by the number of hydrogen bonds formed: the average number per molecule is 4, 2.33, and 2.66 for the 0.96, 0.96-T, and 0.96-T2 networks, respectively. The average (and min/max) O···H distances between adjacent molecules were found to be 2.51 (2.12/3.25), 2.82 (1.92/3.57), and 2.65 (1.80/3.46) Å in the aforementioned networks, respectively. The rotation of the zwitterion also affects the orientation of its molecular dipole, which in turn has an impact on the overall energy as well. These calculations support the structural model for the high-coverage network in a single domain, as illustrated in Figure 1, since the most stable network we have found, and its simulated STM image shown in the SI, matches well with it.

Electronic Structure and Charge Transfer. The charge transfer, which occurs at the metal−molecule interface, is dependent upon the relative energies of the frontier molecular orbitals and the Fermi level (E_F), as well as the overlap between the adsorbate and the surface wave functions.[45] For example, recently we have carried out dispersion-corrected DFT

calculations, which showed that functionalizing benzene with classic activating and deactivating groups can be used to change the magnitude and even the direction of the charge transfer.[27] So, whereas electron density was donated from Cu(111) to 1,3,5-trinitrobenzene, 1,3,5-trimethylbenzene bequeathed some of its charge to the metal surface. Moreover, our prior molecular calculations (which employed a finite cluster to model the surface) revealed that the parent quinonoid zwitterion interacts with Cu(111) and Ag(111) via a transfer of electron density from the highest occupied molecular orbital (HOMO) to the metal surface, followed by back-donation into the lowest unoccupied molecular orbital (LUMO),[15] in the spirit of the Dewar, Chatt, and Duncanson model.[46,47]

To investigate the nature of the charge reorganization upon molecular adsorption to the Au(111) surface in greater detail, we have calculated the charge density difference (CDD) plots for the various coverages considered. The CDD may be obtained by taking the difference between the self-consistent charge density of the interacting system and a sum of the densities of the isolated substrate and adsorbate (but using the geometry as for the interacting system). For low coverages the CDD plot (see Figure 5) illustrates that there is a build-up of electronic charge (red) below the amine-containing side of the zwitterion and a depletion of electronic charge (blue) below the end which contains oxygen, in line with the results previously obtained for adsorption to Cu(111) and Ag(111).[15] The CDD plots show that for all three substrates at low coverage the charge transfer induces a surface dipole which opposes the molecular dipole. The pillow effect[48] dictates that the electron density just above the surface decreases upon adsorption as a result of Pauli repulsion. Regions showing both a depletion and an increase in the charge density between the molecule and the surface are evident at low coverage, suggesting that both Pauli repulsion and charge donation from the molecule are important in explaining the charge redistribution that occurs. A Bader charge analysis of the valence charge density[49] yields a charge per molecule of +0.09e, +0.04e, and +0.02e for the 0.32, 0.64, and 0.96 ML coverages, respectively. Although small, the trend does agree with how increased molecular coverage lowers the adsorbate's interaction with the surface. We have therefore visually inspected the charge density differences calculated for different coverages and from the observed trends infer the likely consequences on the induced surface dipole.

As the coverage increases, so does the surface−adsorbate distance, with a concomitant decrease in the overlap of the molecular and the surface wave functions. Thus, the amount of Pauli repulsion observed at higher coverages ought to be smaller than at lower ones. Indeed, in Figure 6 it appears that at the highest coverage considered, 0.96 ML, the "blue" regions between the surface and the zwitterion are minimal. The CDD plot is indicative of a loss of charge in the π-system of the zwitterions, and there is a small buildup in the plane of the molecule, indicative of $\sigma-\pi$ mixing which occurs as a result of a slight tilting of the anionic part of the molecule toward the surface. This is perhaps seen most clearly in the bottom panel in Figure 7(c). Careful inspection of the CDD plots suggest that for higher coverages the component of the induced surface dipole which lies perpendicular to the surface increases, and the one which is parallel to the surface (opposing the molecular dipole) is decreasing. The depolarization model of Langmuir suggests that the strength of the surface dipoles, which are generated as a result of molecular adsorption, decreases as the number of induced dipoles increases.[50]

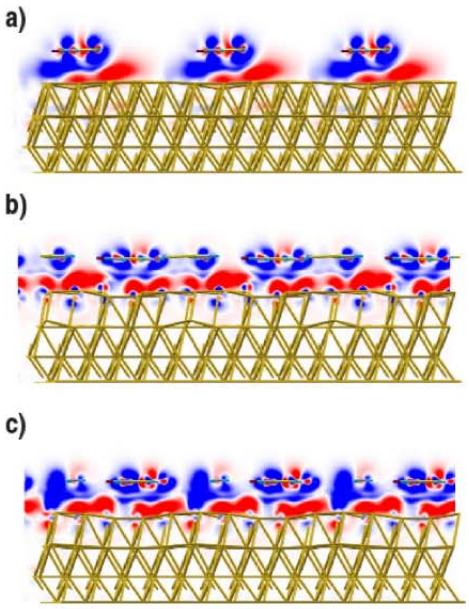

Figure 6. Redistribution of electronic charge which occurs upon adsorption of the zwitterion to the Au(111) surface calculated for coverages of (a) 0.32, (b) 0.64, and (c) 0.96 ML. Red indicates a build-up and blue a depletion of charge. The picture provides a two-dimensional cut of the CDD bisecting the molecule, and the colors representing the isovalues are the same as in Figure 5. Isosurfaces for these CDDs are shown in Figure 7.

To further study how the electronic structure changes upon molecular adsorption, we have plotted the projected densities of states (PDOS) arising from the zwitterion for various coverages and compare them to the energy of the frontier molecular orbitals of the free molecule in Figure 8. At the lowest coverage considered the peak attributed to the HOMO is quite broad, a result of the increased overlap between the molecular and surface MOs, which occurs because of the smaller distance between them (see Table 2). Because of this broadening, the top of the peak crosses the Fermi level, so that the HOMO is not completely occupied. The interaction of the HOMO with the metal surface can give rise to either a four-electron event or a two-electron event. In the case of the former, the HOMO interacts with a filled band, and if the antibonding combination of the two rises above the Fermi level, the electrons will be "dumped" into the surface, thereby relieving the Pauli repulsion.[45,51] In the case of the latter, the interaction is with an unoccupied metal band, but the result is the same: charge is transferred from the molecule to the surface too. It appears that there is very little back-donation to the LUMO, which is located over 1 eV above the Fermi level, in contrast to what was observed for Cu(111) and Ag(111).

Upon increasing coverage, the supramolecular interactions become progressively more important as the intermolecular distances decrease. The distance between the surface and the adsorbate increases, on the other hand, so the peak attributed to the HOMO in the PDOS plots becomes less disperse. The narrowing of this peak, and the shift of the HOMO further away from the Fermi level, results in an increase in the

dx.doi.org/10.1021/jp403384h | J. Phys. Chem. C XXXX, XXX, XXX XXX

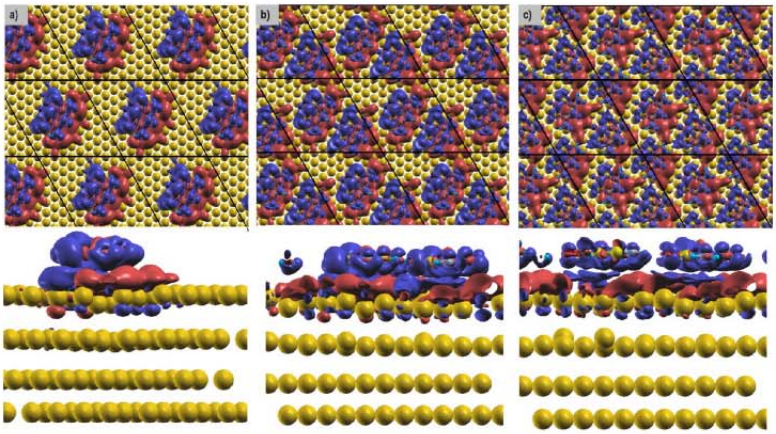

Figure 7. Redistribution of electronic charge which occurs upon adsorption of the zwitterion to the Au(111) surface calculated for (a) 0.32, (b) 0.64, and (c) 0.96 ML coverages. Red indicates a build-up and blue a depletion of charge in these charge density difference (CDD) isosurface plots ($\pm$0.002 e/Å^3). The top panel provides a birds eye view and the bottom panel a side-on view.

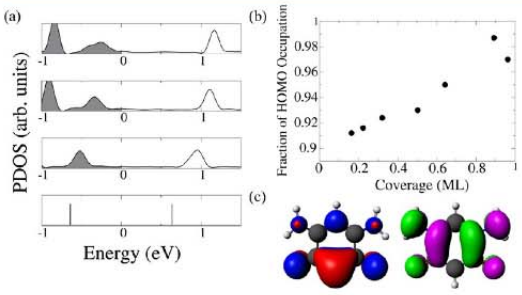

Figure 8. (a) PDOS of the zwitterion at (top to bottom) 0.16 ML, 0.50 ML, and 0.89 ML coverage and the gas phase. The Fermi level has been adjusted to zero. (b) Fraction of occupation of the HOMO as a function of coverage. (c) Isosurface ($\pm$0.03 au) plots of the HOMO/LUMO of the quinonoid zwitterion.

occupation of the HOMO at higher coverages, as illustrated in the right panel in Figure 8. These results are in-line with our Bader charge analysis. Similar trends in the HOMO occupation as a function of coverage have been computed previously, for example, for tetrathiafulvalene on Au(111).[21] It is apparent in the case of these zwitterion molecules that attractive supramolecular interactions (dipole−dipole, H-bonding) are not dampened as a function of coverage, but rather the interaction between the surface and the adsorbate is. Our calculations demonstrate that in this system relatively strong attractive adsorbate−adsorbate interactions dominate over Coulombic repulsion brought about by the charge redistribution which occurs upon molecular adsorption.[52]

■ CONCLUSIONS

At first glance, the experimentally observed self-assembled arrangement of zwitterions on Au(111) bears a striking resemblance to the 2D networks of room-temperature deposited zwitterions on Ag(111) but is vastly different from the 1D hydrogen bonded chains of antiparallel aligned molecules found on Cu(111).[15] However, important differences between the same networks on Ag(111) and Au(111) become observable upon closer inspection of the details of the molecular arrangement with respect to the substrate lattice. Specific for zwitterions on Au(111) is that the 2D adsorbate layer is incommensurate with the Au(111) surface, albeit growth is templated by the densely packed ⟨101⟩ rows of Au. And although the molecules seem to overgrow the herringbone reconstruction of the Au surface unimpeded, the nucleation sites of molecular islands are precisely determined by this reconstruction.

Our first-principles calculations predict that the diffusion barrier of the zwitterions is small for low coverages. This prediction is in agreement with the experimentally observed incommensurate structures. Importantly, the calculations further demonstrate that the interactions of the adsorbates with the substrate, the charge transfer which occurs upon adsorption, and the resulting dipole depend upon the molecular density. As the distance between the molecules decreases with increasing coverage, the intermolecular interaction becomes larger with a concomitant increase in the substrate−adsorbate distance. The result is a decrease of the Pauli repulsion and a reorganization of the charge density which occurs upon molecular adsorption. This in turn affects the induced surface dipole, as well as the overall dipole of the system.

This study therefore shows that organic adsorbate−substrate interactions can be strongly coverage dependent, so that computations performed on a single molecule on a substrate slab may not always be a good model to determine the properties of the metal−organic interface. If the molecules are arranged in a way so that they maximize the number of intermolecular hydrogen bonds in the calculations, the binding energy between them may be quite strong. Especially for this system at high coverage, the tendency of the molecules to form hydrogen bonds clearly dominates over the arrangement of molecular dipoles to minimize the electrostatic energy.

There is a fine balance between intermolecular bonding forces and adsorbate−substrate interaction, which shifts in favor of the former with increasing coverage. This is even seen in the experiment as a slight shortening of the intermolecular bond length at near-full monolayer coverage. This experimental

dx.doi.org/10.1021/jp403384h | J. Phys. Chem. C XXXX, XXX, XXX XXX

observation, however, is surprising. The observed molecular arrangement at low coverage is very different from the arrangement assumed in the theoretical model. In experiment, the molecule distribution is inhomogeneous, with nucleated islands exhibiting high areal density, separated by a large empty space. The theoretical model is based on a homogeneous molecule distribution, where the molecule−molecule bond length is a function of coverage. In this sense, the high-coverage computational models appear to be a better description of the zwitterionic networks adsorbed on Au(111) at all coverages. However, the precise measurements of intermolecular distances with sub-Angstrom resolution show that the bonds do contract slightly, by a mere 0.2 Å, as the islands grow. This is interpreted as an experimental confirmation of the predicted weakening of the molecule−substrate interactions with increasing coverage.

■ ASSOCIATED CONTENT

Supporting Information

Optimized coordinates for each system, simulated STM images, further computational results. This material is available free of charge via the Internet at http://pubs.acs.org.

■ AUTHOR INFORMATION

Corresponding Author

*E-mail: aenders2@unl.edu; ezurek@buffalo.edu.

Notes

The authors declare no competing financial interest.

■ ACKNOWLEDGMENTS

This work was supported by grants DMR-0747704, DMR-0213808, CHE-0909580, and EPS-1004094, the CNRS and the Ministere de la Recherche (Paris). Support from the Center of Computational Research at SUNY Buffalo is acknowledged. E.Z. thanks the Alfred P. Sloan Foundation for a Research Fellowship (2013-2015).

■ REFERENCES

(1) Aviram, A. Molecules for Memory, Logic, and Amplification. *J. Am. Chem. Soc.* **1988**, *110*, 5687−5692.
(2) Narayanan Unni, K. N.; Bettignies, R.; Dabos-Seignon, S.; Nunzi, J. A Nonvolatile Memory Element Based on an Organic Field-effect Transistor. *Appl. Phys. Lett.* **2004**, *85*, 1823−1825.
(3) Yuan, Y.; Reece, T. J.; Sharma, P.; Poddar, S.; Ducharme, S.; Gruverman, A.; Yang, Y.; Huang, J. Efficiency Enhancement in Organic Solar Cells with Ferroelectric Polymers. *Nat. Mater.* **2011**, *10*, 296−302.
(4) Forrest, S. R. The Path to Ubiquitous and Low-Cost Organic Electronic Appliances on Plastic. *Nature* **2004**, *428*, 911−918.
(5) Coratger, R.; Estrampes, N.; Coudret, C. Observation of Anthraquinone Compounds Using Low Temperature Scanning Tunneling Microscopy. *Surf. Sci.* **2007**, *601*, 2277−2283.
(6) Vaughan, O.; Alavi, A.; Williams, F.; Lambert, R. Dipole Amplification: A Principle for the Self-Assembly of Asymmetric Monomers on Metal Surfaces. *Angew. Chem., Int. Ed.* **2008**, *47*, 2422−2426.
(7) Baber, A. E.; Jensen, S. C.; Sykes, E. C. H. Dipole-Driven Ferroelectric Assembly of Styrene on Au(111). *J. Am. Chem. Soc.* **2007**, *129*, 6368−6369.
(8) Kuck, S.; Chang, S.; Klockner, J.; Prosenc, M. H.; Hoffmann, G.; Wiesendanger, R. Steering Two-Dimensional Molecular Growth via Dipolar Interaction. *Chem. Phys. Chem.* **2009**, *10*, 2008−2011.
(9) Gavezzotti, A.; Simonetta, M.; Van Hove, M. A.; Somorjai, G. A. Adsorbate−Adsorbate Interactions and the Ordering of Organic Monolayers on metal surfaces. *Surf. Sci.* **1985**, *154*, 109−120.
(10) Siri, O.; Braunstein, P. Unprecedented Zwitterion in Quinonoid Chemistry. *Chem. Commun.* **2002**, 208−209.
(11) Braunstein, P.; Siri, O.; Taquet, J.; Rohmer, M.; Benard, M.; Welter, R. A $6\pi + 6\pi$ Potentially Antiaromatic Zwitterion Preferred to a Quinoidal Structure: Its Reactivity Toward Organic and Inorganic Reagents. *J. Am. Chem. Soc.* **2003**, *125*, 12246−12256.
(12) Tamboura, F. B.; Cazin, C. S. J.; Pattacini, R.; Braunstein, P. Reactions of Amines with Zwitterionic Quinoneimines: Synthesis of New Anionic and Zwitterionic Quinonoids. *Eur. J. Org. Chem.* **2009**, *20*, 3340−3350.
(13) Yang, Q.; Siri, O.; Braunstein, P. Tunable N-Substitution in Zwitterionic Benzoquinonemonoimine Derivatives: Metal Coordination, Tandemlike Synthesis of Zwitterionic Metal Complexes, and Supramolecular Structures. *Chem.—Eur. J.* **2005**, *11*, 7237−7246.
(14) Fang, Y.; Nguyen, P.; Ivasenko, O.; Aviles, M. P.; Kebede, E.; Askari, M. S.; Ottenwaelder, X.; Ziener, U.; Siri, O.; Cuccia, L. A. Charge-Assisted Hydrogen Bond-Directed Self-Assembly of an Amphiphilic Zwitterionic Quinonemonoimine at the Liquid−Solid Interface. *Chem. Commun.* **2011**, *47*, 11255−11257.
(15) Kunkel, D. A.; Simpson, S.; Nitz, J.; Rojas, G. A.; Zurek, E.; Routaboul, L.; Doudin, B.; Braunstein, P.; Dowben, P. A.; Enders, A. Dipole Driven Bonding Schemes of Quinonoid Zwitterions on Surfaces. *Chem. Commun.* **2012**, *48*, 7143−7145.
(16) Jewell, A. D.; Simpson, S. M.; Enders, A.; Zurek, E.; Sykes, E. C. H. Magic Electret Clusters of 4-Fluorostyrene on Metal Surfaces. *J. Phys. Chem. Lett.* **2012**, 2069−2075.
(17) Perdereau, J.; Biberian, J. P.; Rhead, G. E. Adsorption and Surface Alloying of Lead Monolayers on (111) and (110) Faces of Gold. *J. Phys. F* **1974**, *4*, 798.
(18) Sandy, A. R.; Mochrie, S. G. J.; Zehner, D. M.; Huang, K. G.; Gibbs, D. Structure and Phases of the Au(111) Surface: X-ray-Scattering Measurements. *Phys. Rev. B* **1991**, *43*, 4667−4687.
(19) Barth, J. V.; Brune, H.; Ertl, G.; Behm, R. J. Scanning Tunneling Microscopy Observations on the Reconstructed Au(111) Surface: Atomic Structure, Long-Range Superstructure, Rotational Domains, and Surface Defects. *Phys. Rev. B* **1990**, *42*, 9307−9318.
(20) Woll, C.; Chiang, S.; Wilson, R. J.; Lippel, P. H. Determination of Atom Positions at Stacking-Fault Dislocations on Au(111) by Scanning Tunneling Microscopy. *Phys. Rev. B* **1989**, *39*, 7988−7991.
(21) Fraxedas, J.; Garcia-Gil, S.; Monturet, S.; Lorente, N.; Fernandez-Torrente, I.; Franke, K. J.; Pascual, J. I.; Vollmer, A.; Blum, R.-P.; Koch, N.; et al. Modulation of Surface Charge Transfer through Competing Long-Range Repulsive versus Short-Range Attractive Interactions. *J. Phys. Chem. C* **2011**, *115*, 18640−18648.
(22) Kovacevic, N.; Kokalj, A. DFT Study of Interaction of Azoles with Cu(111) and Al(111) Surfaces: Role of Azole Nitrogen Atoms and Dipole-Dipole Interactions. *J. Phys. Chem. C* **2011**, *115*, 24189−24197.
(23) Pekoz, R.; Johnston, K.; Donadio, D. Adsorption of Dichlorobenzene on Au and Pt Stepped Surfaces Using van der Waals Density Functional Theory. *J. Phys. Chem. C* **2012**, *116*, 20409−20416.
(24) Le, D.; Aminpour, M.; Kiejna, A.; Rahman, T. S. The Role of van der Waals Interaction in the Tilted Binding of Amine Molecules to the Au(111) Surface. *J. Phys.: Condens. Matter* **2012**, *24*, 222001.
(25) Yildirim, H.; Kara, A. Effect of van der Waals Interactions on the Adsorption of Olympicene Radical on Cu(111): Characteristics of Weak Physisorption versus Strong Chemisorption. *J. Phys. Chem. C* **2013**, *117*, 2893−2902.
(26) Liu, W.; Carrasco, J.; Santra, B.; Michaelides, A.; Scheffler, M.; Tkatchenko, A. Benzene Adsorbed on Metals: Concerted Effect of Covalency and van der Waals Bonding. *Phys. Rev. B* **2012**, *86* (245405), 1−6.
(27) Simpson, S.; Zurek, E. Substituted Benzene Derivatives on the Cu(111) Surface. *J. Phys. Chem. C* **2012**, *116*, 12636−12643.
(28) Yang, Q. Z.; Siri, O.; Braunstein, P. First Transamination Reactions for the One-pot Synthesis of Substituted Zwitterionic Quinones. *Chem. Commun.* **2005**, 2660−2662.

(29) Kresse, G.; Hafner, J. *Ab initio* Molecular Dynamics for Liquid Metals. *Phys. Rev. B* **1993**, *47*, 558−561.
(30) Blochl, P. E. Projector Augmented-Wave Method. *Phys. Rev. B* **1994**, *50*, 17953−17979.
(31) Lee, K.; Murray, E. D.; Kong, L.; Lundqvist, B. I.; Langreth, D. C. Higher-Accuracy van der Waals Density Functional. *Phys. Rev. B* **2010**, *82*, 081101.
(32) Klimes, J.; Bowler, D. R.; Michaelides, A. Van der Waals Density Functionals Applied to Solids. *Phys. Rev. B* **2011**, *83* (195131), 1−13.
(33) Garcia-Lastra, J. M.; Rostgaard, C.; Rubio, A.; Thygesen, K. S. Polarization-Induced Renormalization of Molecular Levels at Metallic and Semiconducting Surfaces. *Phys. Rev. B* **2009**, *80*, 245427.
(34) Dion, M.; Rydberg, H.; Schroder, E.; Langreth, D. C.; Lundqvist, B. I. Van der Waals Density Functional for General Geometries. *Phys. Rev. Lett.* **2004**, *92* (246401), 1−4.
(35) Berland, K.; Einstein, T. L.; Hyldgaard, P. Rings Sliding on a Honeycomb Network: Adsorption Contours, Interactions, and Assembly of Benzene on Cu(111). *Phys. Rev. B* **2009**, *80*, 155431.
(36) Chen, D. L.; Al-Saidi, W. A.; Johnson, J. K. The Role of van der Waals Interactions in the Adsorption of Noble Gases on Metal Surfaces. *J. Phys.: Condens. Matter* **2012**, *24* (424211), 1−10.
(37) Lee, K.; Berland, K.; Yoon, M.; Andersson, S.; Schroder, E.; Hyldgaard, P.; Lundqvist, B. I. Benchmarking van der Waals Density Functionals with Experimental Data: Potential-Energy Curves for H2 Molecules on Cu(111), (100) and (110) Surfaces. *J. Phys.: Condens. Matter* **2012**, *24* (424213), 1−15.
(38) Klimes, J.; Michaelides, A. Perspective: Advances and Challenges in Treating van der Waals Dispersion Forces in Density Functional Theory. *J. Chem. Phys.* **2012**, *137* (120901), 1−12.
(39) Kunkel, D. A.; Hooper, J.; Simpson, S.; Rojas, G. A.; Ducharme, S.; Usher, T.; Zurek, E.; Enders, A. Proton Transfer in Surface-Stabilized Chiral Motifs of Croconic Acid. *Phys. Rev. B.* **2013**, *87* (041402), 1−4.
(40) Syomin, D.; Kim, J.; Koel, B.; Ellison, G. B. Identification of Adsorbed Phenyl (C6H5) Groups on Metal Surfaces: Electron-Induced Dissociation of Benzene on Au(111). *J. Phys. Chem. B* **2001**, *105*, 8387−8394.
(41) Rockey, T. J.; Yang, M.; Dai, H.-L. Adsorption Energies, Inter-Adsorbate Interactions, and the Two Binding Sites within Monolayer Benzene on Ag (111). *J. Phys. Chem. B* **2006**, *110*, 19973−19978.
(42) Ruiz, V. G.; Liu, W.; Zojer, E.; Scheffler, M.; Tkatchenko, A. Density-Functional Theory with Screened van der Waals Interactions for the Modeling of Hybrid Inorganic-Organic Systems. *Phys. Rev. Lett.* **2012**, *108* (146103), 1−5.
(43) Kepcija, N.; Zhang, Y. Q.; Kleinschrodt, M.; Bjork, J.; Klyatskaya, S.; Klappenberger, F.; Ruben, M.; Barth, J. V. Steering On-Surface Self-Assembly of High-Quality Hydrocarbon Networks with Terminal Alkynes. *J. Phys. Chem. C* **2013**, *117*, 3987−3995.
(44) Tomba, G.; Stengel, M.; Schneider, W. D.; Baldereschi, A.; De Vita, A. Supramolecular Self-Assembly Driven by Electrostatic Repulsion: The 1D Aggregation of Rubrene Pentagons on Au(111). *ACS Nano* **2010**, *4*, 7545−7551.
(45) Hoffmann, R. A Chemical and Theoretical Way to Look at Bonding on Surfaces. *Rev. Mod. Phys.* **1988**, *60*, 601−628.
(46) Dewar, M. J. S. *Bull. Soc. Chim. France* **1951**, *18*, C79.
(47) Chatt, J.; Duncanson, L. A. Olefin Co-ordination Compounds. Part III. Infra-red Spectra and Structure: Attempted Preparation of Acetylene Complexes. *J. Chem. Soc.* **1953**, 2939−2947.
(48) Bagus, P. S.; Staemmler, V.; Woll, C. Exchangelike Effects for Closed-Shell Adsorbates: Interface Dipole and Work Function. *Phys. Rev. Lett.* **2002**, *89* (096104), 1−4.
(49) (a) Rodríguez, J. I.; Bader, R. F. W.; Ayers, P. W.; Michel, C.; Gotz, A. W.; Bo, C.. A High Performance Grid-Based Algorithm for Computing QTAIM Properties. *Chem. Phys. Lett.* **2009**, *472*, 149−152. (b) Tang, W.; Sanville, E.; Henkelman, G. A Grid-Based Bader Analysis Algorithm Without Lattice Bias. *J. Phys.: Condens. Matter* **2009**, *21*, 084204.
(50) Langmuir, I. Vapor Pressures, Evaporation, Condensation and Adsorption. *J. Am. Chem. Soc.* **1932**, *54*, 2798−2832.
(51) Philipsen, P. H.; Baerends, E. J. Role of the Fermi Surface in Adsorbate−Metal Interactions: An Energy Decomposition Analysis. *J. Phys. Chem. B* **2006**, *110*, 12470−12479.
(52) Rojas, G.; Simpson, S.; Chen, X.; Kunkel, D. A.; Nitz, J.; Xiao, J.; Dowben, P. A.; Zurek, E.; Enders, A. Surface State Engineering of Molecule−Molecule Interactions. *Phys. Chem. Chem. Phys.* **2012**, *14*, 4971−4976.